



Constraining the Rate of Primordial Black Hole Explosions and Extra-Dimension Scale
Using a Low-Frequency Radio Antenna Array

Author(s): Sean E. Cutchin, John H. Simonetti, Steven W. Ellingson, Amanda S.
Larracuenta and Michael J. Kavic

Source: *Publications of the Astronomical Society of the Pacific*, Vol. 127, No. 958
(December 2015), pp. 1269-1278

Published by: Astronomical Society of the Pacific

Stable URL: <https://www.jstor.org/stable/10.1086/684195>

Accessed: 15-01-2023 21:27 UTC

JSTOR is a not-for-profit service that helps scholars, researchers, and students discover, use, and build upon a wide range of content in a trusted digital archive. We use information technology and tools to increase productivity and facilitate new forms of scholarship. For more information about JSTOR, please contact support@jstor.org.

Your use of the JSTOR archive indicates your acceptance of the Terms & Conditions of Use, available at
<https://about.jstor.org/terms>



JSTOR

Astronomical Society of the Pacific is collaborating with JSTOR to digitize, preserve and extend access to *Publications of the Astronomical Society of the Pacific*

Constraining the Rate of Primordial Black Hole Explosions and Extra-Dimension Scale Using a Low-Frequency Radio Antenna Array

SEAN E. CUTCHIN,¹ JOHN H. SIMONETTI,¹ STEVEN W. ELLINGSON,² AMANDA S. LARRACUENTE,³ AND MICHAEL J. KAVIC³

Received 2014 September 10; accepted 2015 September 19; published 2015 November 2

ABSTRACT. An exploding primordial black hole (PBH) may produce a single pulse of electromagnetic radiation detectable at the low-frequency end of the radio spectrum. Furthermore, a radio transient from an exploding PBH could be a signature of an extra spatial dimension. We describe here an approach for searching for PBH explosions using a low-frequency radio antenna array, and as a practical example, the results of such a search using the Eight-meter-wavelength Transient Array (ETA). No compelling astrophysical signal was detected in ≈ 4 hr of data, implying an observational upper limit on the rate of exploding PBHs is $2.3 \times 10^{-7} \text{ pc}^{-3} \text{ yr}^{-1}$ for an exploding PBH with a fireball Lorentz factor of $10^{4.3}$ for the standard scenario of Page and Hawking. This rate limit is the strongest constraint yet set for PBH explosions with this fireball Lorentz factor. Observations (~ 300 hr) using the Arecibo Observatory were used to set a stronger constraint on the rate of PBH explosions for a fireball Lorentz factor of $10^{4.6}$, but the limit set by those observations for the fireball Lorentz factor considered here are less stringent by more than an order of magnitude. The limits considered here are applicable to exploding PBHs in the halo of the Galaxy. These observations also imply an upper limit of $2.3 \times 10^{-4} \text{ pc}^{-3} \text{ yr}^{-1}$ on the rate of PBH explosions in the context of certain extra dimension models, as described by Kavic et al. This rate limit is for a fireball Lorentz factor of $10^{4.3}$, which corresponds to an extra dimension compactification scale of $5.0 \times 10^{-18} \text{ m}$.

1. INTRODUCTION

The study of black holes underpins much of modern astrophysics. In 1975, Hawking suggested that black holes emit energy like blackbodies with a temperature inversely proportional to the black hole mass (Hawking 1975). Thus, black holes evaporate, and the rate of evaporation is greater for smaller-mass black holes. While the evaporation rate for stellar-mass black holes is too low to imply practical observable consequences, small enough black holes could completely evaporate on a time-scale comparable to the age of the universe. Such small-mass black holes produced by the big bang—primordial black holes (PBHs)—could now be reaching their endpoints and perhaps explode during their final moments. Observing these explosions would be of obvious cosmological and physical significance.

Page and Hawking predicted that an evaporating primordial black hole would explode, releasing a final burst of energy upon reaching the QCD energy scale at $kT \sim 0.1 \text{ GeV}$ (where T is the temperature of the black hole), producing a burst of gamma rays (Page & Hawking 1976). The Energetic Gamma-Ray Experiment Telescope (EGRET) set an upper limit on PBH explosions of $< 0.059 \text{ pc}^{-3} \text{ yr}^{-1}$ (Lehoucq et al. 2009), assuming the

gamma-ray spectrum peaks at about 250 MeV, as discussed by Page and Hawking.

However, there is another way to search for exploding PBHs that can yield better limits, as first pointed out by Rees (1977). A “fireball” of relativistic charged particles ejected by the explosion (e.g., electron-positron pairs) would act as a superconducting, expanding shell and expel the ambient interstellar magnetic field from a spherical volume centered on the exploding PBH, producing a radio pulse potentially detectable at large interstellar distances. Given the spectrum of radio emission derived by (Blandford 1977), a low-frequency radio search can set better limits than gamma-ray searches.

A number of radio searches, mainly using single-dish telescopes, have yielded PBH explosion limits, some of which are better than obtained by gamma-ray searches. In particular, one search by Phinney & Taylor (1979), using ~ 300 hr of observing time on the Arecibo telescope, claimed a limit of $2 \times 10^{-9} \text{ pc}^{-3} \text{ yr}^{-1}$. However, this limit was based on the incorrect assumption of a flat radio pulse spectrum across the observing bandwidth. When the spectrum derived by Blandford (1977) is used, the constraint becomes $1.1 \times 10^{-8} \text{ pc}^{-3} \text{ yr}^{-1}$ for a fireball Lorentz factor of $10^{4.6}$. The current work sets the strongest constraint on the PBH explosion rate limit for a Lorentz factor of $10^{4.3}$. The Arecibo observations noted above can be used to set a PBH explosion rate limit for a 5σ detection threshold of $4.8 \times 10^{-6} \text{ pc}^{-3} \text{ yr}^{-1}$ for this fireball Lorentz factor, which is more than an order of magnitude less stringent than the limit set here. As discussed below,

¹ Department of Physics, Virginia Polytechnic Institute and State University, Blacksburg, VA 24061.

² Bradley Department of Electrical and Computer Engineering, Virginia Polytechnic Institute and State University, Blacksburg, VA 24061.

³ Department of Physics, Long Island University, Brooklyn, NY 11201.

the different values of the Lorentz factor correspond to different assumptions about either the particle spectrum at the QCD scale or the compactification scale of an extra spatial dimension, depending on the model being considered. Note that the rate limits noted above are for the traditional PBH explosion model due to Page & Hawking (1976). It is also worth noting that these limits apply to an arcminute (approximately) beam of great depth, extending well beyond radius of the Galaxy. This is further discussed in § 5.

In this article, we demonstrate how a low-frequency radio antenna array instantaneously sensitive to a large fraction of the sky above the horizon can be used to conduct such a search that easily surpasses the limits set with single-dish telescopes. Unlike the Arecibo search, a search using a low-frequency antenna array such as described here would only be sensitive to exploding PBHs within our Galaxy or perhaps the Galactic halo; it has been suggested that PBHs can be highly concentrated in galaxies, specifically in the Galactic halo (Wright 1996).

Low-frequency antenna arrays have been used to search for radio transients for many years (Jelley et al. 1965; Porter et al. 1965; Balsano et al. 1996). However, the commissioning of a new generation of low-frequency arrays (Ellingson et al. 2007; Taylor et al. 2012; Stappers et al. 2011; Tingay et al. 2013) in combination with the development of a new class of source models for radio transient production, including novel PBH emission mechanisms (Kavic et al. 2008; Barrau et al. 2014), suggest we re-examine our ability to use such arrays to search for transient signals. New developments in hardware and data processing techniques allow this new class of instruments to search for radio transients with greater sensitivity than ever before. Data from current arrays such as the first station of the Long Wavelength Array (LWA1) (Taylor et al. 2012) and the Low Frequency Array for radio astronomy (LOFAR) (Stappers et al. 2011) can be searched for signals more effectively and with increased resolution than earlier instruments. We present the results of such a search we conducted using a small array of antennas that served as a pathfinder for the LWA1, the Eight-meter-wavelength Transient Array (ETA) (Ellingson et al. 2007). While the limit set by the observations presented is the strongest constraint available for a limited range of fireball Lorentz factors, further observations with the LWA1 or LOFAR would extend this work and set the most stringent limits to date for all possible fireball Lorentz factors.

In addition to the “standard” exploding PBH scenario of Page & Hawking (1976), Kavic et al. (2008) have recently pointed out that there is a second and observationally distinct explosion scenario, in this case for a PBH in the presences of an extra spatial dimension. In short, an evaporating black hole in the presence of an extra spatial dimension would undergo a black-string-to-five-dimensional-black-hole phase transition that could produce an explosive transient event. This topological phase-transition explosion could also produce a detectable radio signal. We will compute possible limits obtainable using

an antenna array for exploding PBHs in the standard scenario and the topological phase-transition scenario. The constraints on the scale of an extra dimension that are presented here are entirely novel. These constraints represent a truly modern method of using low-frequency arrays to search for exotic phenomena.

This paper is organized as follows: § 2 describes the two PBH explosion scenarios considered. § 3 discusses ETA, observations, and our data reduction procedure. § 4 presents observational limits on the PBH explosion rate. Finally, we discuss the implications of our search in § 5.

2. EXPLOSIVE PBH SCENARIOS

2.1. Standard Scenario of Page and Hawking

Hawking suggested that a black hole emits energy like a blackbody (Hawking 1975) with the temperature defined as

$$T = \frac{\hbar c^3}{8\pi G k M}, \quad (1)$$

where M is the mass of the black hole. The emitted energy comes at the expense of the black hole’s mass, and as its mass decreases, its temperature and mass loss rate increase. Since a black hole radiates like a blackbody, the emitted power is

$$P = 4\pi R_s^2 \alpha(T) T^4, \quad (2)$$

where R_s is the Schwarzschild radius, and $\alpha(T)$ is proportional to the number of particle modes available at the temperature T . At very low temperatures, where kT is less than the energy of any particle of nonzero mass, the only particles that can be emitted are photons, and α is equal to the Stefan–Boltzmann constant, $\alpha = \sigma = \pi^2 k^4 / 60 \hbar^3 c^2$. At higher temperatures, a spectrum of photons and particles of nonzero mass will be emitted. The emitted energy comes at the expense of the black hole’s mass. Thus,

$$-\frac{dM}{dt} c^2 = 4\pi R_s^2 \alpha(T) T^4 \propto \frac{1}{M^2}. \quad (3)$$

Page & Hawking (1976) described the explosion for a scenario in which all the remaining mass is emitted in a burst of energy Mc^2 near the QCD energy scale, $kT \sim 0.1$ GeV.

2.2. Topological Phase-Transition Scenario

Kol (2002) discussed a scenario whereby a compactified extra spatial dimension could produce a black hole explosion. This scenario was considered in the context of PBH evaporation in Kavic et al. (2008). Black holes in four dimensions are uniquely defined by charge, mass, and angular momentum. However, with the addition of an extra spatial dimension, black holes could exist in different phases and undergo phase transitions.

For one toroidally compactified extra dimension, two possible phases are a “black string” wrapping the compactified extra dimension and a five-dimensional black hole smaller than the extra dimension.

When a PBH is larger in size than the extra dimension, it wraps the extra dimension to form a black string, and as the PBH evaporates, it will eventually reach a radius comparable to the size of the extra spatial dimension. The “width” of the string is decreasing as the object evaporates, while the “length” of the string is still wrapped around the extra dimension. This situation is unstable (Gregory & Laflamme 1993), and the string should eventually snap, allowing the object to shrink to a size that can fit within the extra spatial dimension. On “snapping,” the black hole releases a few percent of its mass-energy in an explosion of timescale L/c , where L is the size of the extra spatial dimension. The phase transition from black string to black hole is expected to occur at a dimensionless (mass) parameter of $\mu \approx 0.07$, where $\mu = GM/Lc^2$. The mass-energy emitted by the object is

$$\eta Mc^2 = \eta \mu Lc^4/G, \quad (4)$$

where $\eta \approx 0.02$ is the efficiency (Kol 2002).

It is important to note that these two scenarios are mutually exclusive as the extra-dimensional scenario would preclude a radio burst associated with the terminal outburst of the PBH, as described in the standard scenario. This is because, following the black-string-to-black-hole phase transition, evaporation takes place in five-dimensional space, and thus the power emitted is reduced, as described by Kol (2002). It should also be noted that a variety of models predict the existence of a single large extra spatial dimension. This includes universal extra dimension models (UED), which predict a compactification scale of $\sim 10^{-18}$ m, as required by Kavic et al. (2008) for radio pulse production.

2.3. Radio Pulse Production

Rees pointed out that searches for the coherent radio pulse that may be generated by the explosion of a black hole would be more sensitive than searches for the emitted burst of Hawking radiation gamma rays (Rees 1977). We discuss here a rough idea of what is happening in this radio pulse production. The detailed properties of this pulse were discussed by Blandford (1977), and this analysis was later applied to the extra dimension scenario by Kavic et al. (2008). For the purposes of clarity and completeness, we summarize their results below.

It is assumed that some substantial fraction of the mass-energy emitted in the explosion is in the form of electron-positron pairs. Nearly all of this energy, mc^2 , is in the form of kinetic energy of the emitted particles (i.e., their Lorentz factors are $\gg 1$). The particles form an outwardly expanding thin shell with an expansion speed v (which is constant in this simple discussion), corresponding to a Lorentz factor γ_f . The Lorentz

factor of this expanding “fireball” is taken to be the typical Lorentz factor of the particles. In the case of electron-positron pairs, each pair will typically receive energy kT , thus each particle will end up with a Lorentz factor of

$$\gamma_f = \frac{(1/2)kT}{m_e c^2} = \frac{\hbar c}{16\pi G m_e} \frac{1}{M} \approx 10^5 \left(\frac{10^{11} g}{M} \right), \quad (5)$$

where M is the mass of the black hole at the moment of the explosion.

Since the expanding shell consists of charged particles, the ambient interstellar magnetic field energy is evacuated from the expanding bubble, ejected as electromagnetic radiation. In other words, the shell acts like an expanding, perfectly conducting sphere. The energy of the ambient magnetic field is boosted by γ_f^2 by being reflected off the expanding shell. The expansion ends when the expanding shell reaches a critical radius, R_c , at which the ejected magnetic energy is equivalent to the energy emitted in the explosion.

Only a particular range of γ_f can produce an electromagnetic pulse. The details are discussed by Rees (1977) and by Blandford (1977). Simple arguments can be made for the upper and lower limits of γ_f , which illustrate a few of the processes taken into account in the papers. Below $\gamma_f \sim 10^5$, the energy emitted by the PBH goes primarily into sweeping up the ambient interstellar plasma and not into an electromagnetic pulse; above $\gamma_f \sim 10^7$, the number of electron-positron pairs is insufficient to carry the fireball surface current necessary to expel the interstellar magnetic flux density.

The validity of the Rees model (Rees 1977) was questioned in MacGibbon & Carr (1991). These authors use the standard model of particle physics as a basis for PBH emission at higher temperatures, not the Hagedorn spectrum required by Rees, and thus assume the black hole emits quarks and gluons as predicted by standard QCD models. This analysis leads to the conclusion that a weak burst of gamma rays will result and not a coherent radio signal. A determination of which approach is correct depends chiefly on the physics of the QCD scale. It has been suggested that current experimental data are indicative of a Hagedorn spectrum at the QCD scale (Broniowski et al. 2004), which would lend credibility to the scenario described by Rees, while others disagree with this conclusion (Cohen & Krejcirik 2012). In the current work, we simply constrain the density of PBHs, assuming the Rees model as originally stated. Moreover, the extra dimension scenario also considered here has no dependence on QCD-scale physics and is not addressed in MacGibbon & Carr (1991). Thus, the objections raised do not apply. The search described here yielded no positive detections, and thus we are able to set constraints on both models: on the density of PBHs in the first case and on the density of PBHs and the compactification scale of extra spatial dimensions in the second.

Blandford worked out the details of the spectrum of an emitted radio pulse (Blandford 1977). The discussion below is based on his paper and is used here to analyze the topological phase-transition scenario. However, this analysis also applies to the standard Rees PBH explosion scenario with $\eta = 1$ (Rees 1977). Using equation (5) for the fireball Lorentz factor for a black hole of mass M , the maximum energy that can be released is

$$Mc^2 = \frac{\hbar c^3}{16\pi G m_e} \gamma_f^{-1}. \quad (6)$$

For a topological phase-transition scenario, only a fraction of this mass-energy will be released. Of the released energy, only a fraction will be put into charged particles. The energy released in charged particles (and ultimately into the electromagnetic pulse) is

$$E_{23} \approx \eta_{01} \gamma_{f5}^{-1}, \quad (7)$$

where $\eta_{01} = \eta/0.01$, $\gamma_{f5} = \gamma_f/10^5$, and $E_{23} = E/10^{23}$ J. In equation (7), the nominal value of 0.01 for the efficiency parameter η reflects *both* the expected few-percent efficiency of the mass-energy release by the phase transition *and* the assumption that $\sim 50\%$ of that energy is in the form of relativistic electron-positron pairs.⁴

Using equation (4), we can relate the size of the extra dimension is to the Lorentz factor

$$L \approx \mu_{07}^{-1} \gamma_{f5}^{-1} 10^{-18} \text{ m}, \quad (8)$$

where $\mu_{07} = \mu/0.07$. This relation is used in § 4 to constrain the size of a possible extra dimension in the context of the topological phase-transition scenario.

The fireball expansion timescale ($\approx R_c/c$), given Blandford's results (Blandford 1977), is

$$\Delta t_f = E_{23}^{1/3} \gamma_{f5}^{-2/3} b^{-2/3} 0.60 \text{ s}, \quad (9)$$

which, combined with equation (7), yields

$$\Delta t_f = \eta_{01}^{1/3} \gamma_{f5}^{-1} 0.60 \text{ s}. \quad (10)$$

The critical frequency of the electromagnetic radiation produced by the fireball, following Blandford, is

$$\nu_c = E_{23}^{-1/3} \gamma_{f5}^{8/3} b^{2/3} 5.1 \times 10^9 \text{ Hz}, \quad (11)$$

⁴ Blandford (1977) states that up to $\sim 50\%$ of the released energy might be in the form of electron-positron pairs, but his final numerical results do not explicitly take into account this factor. Benz & Paesold (1998) utilize Blandford's results without explicitly taking into account this factor. Here, we have derived numerical results using $\eta \approx 0.01$, which assumes that 50% of the released energy is in the form of relativistic electron-positron pairs, and ultimately goes into the electromagnetic pulse.

where $b = \mathfrak{B} \sin \theta / 0.5 \times 10^{-9} \text{ T}$ is a magnetic field parameter, \mathfrak{B} is the magnitude of the magnetic flux, and θ is the direction to the observer from the black hole, in standard spherical coordinates, where the z -axis runs along the direction of the magnetic flux. Combining equations (7) and (11) we get

$$\nu_c = \eta_{01}^{-1/3} \gamma_{f5}^3 b^{2/3} 5.1 \times 10^9 \text{ Hz}. \quad (12)$$

From Blandford (1977), the observed pulse energy spectrum (energy per unit frequency interval per unit steradian) is

$$I_{\nu\Omega} = 1.4 \times 10^{12} E_{23}^{4/3} \gamma_{f5}^{-8/3} b^{-2/3} \left| F\left(\frac{\nu}{\nu_c}\right) \right|^2 \text{ J Hz}^{-1} \text{ sr}^{-1}, \quad (13)$$

where

$$F(x) = \int_0^\infty dy y \exp \left[ix \left(y + \frac{y^4}{2} + \frac{y^7}{7} \right) \right]. \quad (14)$$

The limiting forms of $|F(x)|^2$ are

$$|F(x)|^2 = \begin{cases} 0.615 x^{-4/7} - 0.514 x^{-1/7} + 0.027 x^{2/7} \\ \quad + 0.037 x^{5/7} + \mathcal{O}(x^{8/7}) & \text{if } x \lesssim 0.1. \\ x^{-4} (1 - 75,600 x^{-6} + \dots) & \text{if } x \gtrsim 10 \end{cases} \quad (15)$$

Note that $I_{\nu\Omega}$ is the energy per unit frequency interval per steradian, and $I_{\nu\Omega} = 2\pi I_{\omega\Omega}$, where $I_{\omega\Omega}$ is the energy emitted per *angular* frequency interval per steradian (the result Blandford [1977] produced).

Therefore, equations (7) and (13) yield

$$I_{\nu\Omega} = 1.4 \times 10^{12} \eta_{01}^{4/3} \gamma_{f5}^{-4} b^{-2/3} \left| F\left(\frac{\nu}{\nu_c}\right) \right|^2 \text{ J Hz}^{-1} \text{ sr}^{-1}. \quad (16)$$

Observations of a pulse of a specific Lorentz factor (i.e., observations of a specific observed spectrum) can be pinned to a particular efficiency factor if the distance to the explosion can be determined (e.g., through the dispersion measure, in the case of a radio pulse). Thus the “standard” explosion scenario ($\eta \approx 1$) and the topological phase-transition scenario ($\eta \sim 0.01$) can be distinguished. This idea is discussed further by Kavic et al. (2008). In the latter scenario, knowing γ_f implies L . A Lorentz factor of 10^5 corresponds to an extra spatial dimension of $\approx 10^{-18}$ cm, or an energy scale of $kT \approx (\gamma_f/10^5) 0.1 \text{ TeV}$, the electroweak energy scale. The mass of the black hole at the moment of the phase transition is about $10^8 (\gamma_f/10^5)^{-1} \text{ kg}$.

3. OBSERVATIONS AND DATA REDUCTION

3.1. General Considerations

To calculate the observed signal-to-noise ratio, first assume the pulse is not dispersed or scattered. For an explosion at

distance d , detected by a single dipole of collecting area A , using a bandwidth B and integration time τ , the detected signal in units of energy is

$$S = \begin{cases} I_{\nu\Omega} \frac{BA}{d^2} & \text{for } \tau = \Delta t \\ I_{\nu\Omega} \frac{BA}{d^2} \frac{\tau}{\Delta t} & \text{for } \tau < \Delta t \end{cases} \quad (17)$$

This assumes the full bandwidth is detected coherently, and we have assumed the dipole matches the linear polarization of the arriving pulse (the pulse is $\approx 100\%$ linearly polarized since the interstellar magnetic field should be essentially uniform on the length scale R_c). We do not consider the case $\tau > \Delta t$ since the general data analysis procedure is to start with the highest temporal resolution time series and then smooth it, increasing τ until it matches Δt , yielding the highest signal-to-noise ratio for a pulse for this matched situation.

The rms temperature measurement for a radiometer is given by the so-called “radiometer equation,”

$$\sigma_T \approx \frac{T_{\text{sys}}}{\sqrt{B\tau}}, \quad (18)$$

for system temperature T_{sys} , bandwidth B , and integration time τ . The power in noise is $k\sigma_T B$. If we measure the pulse signal in units of energy, the corresponding noise should also be in energy units. As discussed by Meikle & Colgate (1978), the noise N in units of energy, for integration τ , is the noise power multiplied by τ , or

$$N \approx \frac{kT_{\text{sys}}B}{\sqrt{B\tau}} \tau \approx kT_{\text{sys}}\sqrt{B\tau}. \quad (19)$$

Here, the full bandwidth is used in the measurement of the signal. T_{sys} depends on the Local Sidereal Time of the ETA observation and varies between about 6000 and 10,000 K.

The signal-to-noise ratio is therefore

$$\frac{S}{N} \approx \begin{cases} I_{\nu\Omega} \frac{BA}{d^2} \frac{1}{kT_{\text{sys}}\sqrt{B\tau}} & \text{for } \tau \geq \Delta t \\ I_{\nu\Omega} \frac{BA}{d^2} \frac{1}{kT_{\text{sys}}\sqrt{B\tau}} \frac{\tau}{\Delta t} & \text{for } \tau < \Delta t \end{cases} \quad (20)$$

The best S/N is obtained for $\tau = \Delta t$, which is when τ is as small as possible without cutting off some signal from the integration. For N_{dipoles} -independent dipoles, if the resulting time series are added together incoherently, the final signal-to-noise ratio is $(N_{\text{dipoles}}/2)^{1/2}$ better than the single dipole result [the $(1/2)^{1/2}$ comes in since the source is linearly polarized]. In practice, our τ will be set during the data analysis, as we integrate the data over a series of time samples. We will be trying a range of τ in an attempt to match τ to the duration of a pulse buried in the data.

3.2. Interstellar Dispersion, Scattering, and Signal-to-Noise Ratio

Both interstellar dispersion and interstellar scattering may be important in determining the observed pulse duration. In general, the observed pulse duration is

$$\Delta t_{\text{obs}} \approx \sqrt{\Delta t_D^2 + \Delta t_{\text{scatt}}^2}, \quad (21)$$

where Δt_{obs} is the observed pulse width, Δt_D is the pulse broadening due to dispersion, and Δt_{scatt} is the pulse broadening due to scattering. Strictly, equation (21) should include the intrinsic pulse width and observed pulse width contribution from an error in the observed dispersion measure (DM), both added in quadrature within the square root. However, the intrinsic pulse width is negligibly small, being on the order of a nanosecond (it is the inverse of the critical frequency given by eq. [11]), and the DM error can be reduced by decreasing the DM step size in the DM search. So, these two terms are neglected in this discussion.

We will first consider the effect of interstellar dispersion. Break the bandwidth B up into n frequency channels, each of width $\Delta\nu = B/n$. We will incoherently dedisperse a pulse by shifting and adding these channels together, compensating for the relative delay between each channel. For a dispersed pulse, after appropriate dedispersion and summing of the channels, we obtain the same S/N as in the no-dispersion case, as long as the pulse is not smeared in any one channel to a time duration longer than a time sample. In other words, for best signal-to-noise ratio, match τ to the dispersed pulse duration.

At some particular frequency channel, of width $\Delta\nu$, a pulse of originally infinitesimal duration will be spread in time to duration

$$\Delta t_D = \left(\frac{dt}{d\nu} \right)_D \Delta\nu \quad (22)$$

$$= (0.15 \text{ s}) \text{ DM} \left(\frac{\nu}{38 \text{ MHz}} \right)^{-3} \left(\frac{\Delta\nu}{\text{MHz}} \right) \quad (23)$$

$$= (0.11 \text{ s}) \left(\frac{\text{DM}}{50 \text{ pccm}^{-3}} \right) \left(\frac{\nu}{38 \text{ MHz}} \right)^{-3} \left(\frac{\Delta\nu}{15 \text{ kHz}} \right), \quad (24)$$

where $\text{DM} = \int n_e dl$ is the line-of-sight integral of the free electron density n_e . After dedispersion and summing,

$$\frac{S}{N} \approx I_{\nu\Omega} \frac{BA}{d^2} \frac{1}{kT_{\text{sys}}\sqrt{B\Delta t_D}}, \quad (25)$$

assuming the integration time is matched to Δt_D , yielding the best signal-to-noise ratio.

Interstellar scattering can also broaden the pulse. From Cordes & McLaughlin (2003), we can obtain a model of pulse scatter broadening as a function of DM. Matching τ to the final

Δt provides the largest S/N, of course. But τ may have to be large. The scatter-broadened pulse duration is approximately

$$\log\left(\frac{\Delta t_{\text{scatt}}}{\text{seconds}}\right) \approx -9.72 + 0.411 \log \text{DM} + 0.937(\log \text{DM})^2 - 4.4 \log \nu_{\text{GHz}} \pm 0.65, \quad (26)$$

where DM is in units of pc cm^{-3} . For a $\text{DM} \sim 30 \text{ pc cm}^{-3}$, the scatter broadening time is on the order of a few tenths of a second at 38 MHz. At 38 MHz, the diffractive scintillation (twinkling) is “quenched” (smoothed out) in our $\Delta\nu$ frequency channels because the so-called “diffractive scintillation bandwidth” is much less than $\Delta\nu = B/n$, so only scatter broadening of a pulse will affect S/N. The diffraction scintillation bandwidth is $\Delta\nu_{\text{diff}} \sim 1/2\pi\Delta t_{\text{scatt}}$ (Cordes & Rickett 1998), or $\sim 1 \text{ Hz}$ for a Δt_{scatt} that is a few tenths of a second; therefore, $\Delta\nu_{\text{diff}}$ is much less than $\Delta\nu$ (7.32 kHz, for our ETA observations; see below).

Finally, matching the integration time τ to the pulse duration and adding the signals incoherently from N_{dipoles} independent dipoles, the resulting signal-to-noise ratio is

$$\frac{S}{N} \approx I_{\nu\Omega} \frac{BA}{d^2} \frac{1}{kT_{\text{sys}}\sqrt{B\Delta t_{\text{obs}}}} \sqrt{\frac{N_{\text{dipoles}}}{2}}. \quad (27)$$

For an array of dipoles, one could add the dipole signals coherently, i.e., to form a beam, but that beam would necessarily cover a smaller part of the sky than is observed by each dipole. Given that we do not know, in advance, the direction of the incoming radio pulse, the best search scenario should use the widest beam possible. Thus, we chose to add the signals incoherently, producing equation (27).

3.3. ETA Observations

Data for the current work were collected with the ETA in five observing sessions between 2007 November 18 and 2007 December 3.⁵ The observing sessions lasted between 30 minutes and 1 hr. For a full description of ETA, see Ellingson et al. (2007) and Deshpande (2009). ETA was designed to provide roughly uniform sensitivity over most of the visible sky. It consisted of 12 dual-polarized dipole antennas that operated in the band of 29–47 MHz. All data sets were taken with ETA at 38 MHz frequency with a 3.75 MHz processed bandwidth. ETA parameters relevant to this observation are listed in Table 1. Note, in particular, that only four dipoles were used in these observations. Following the analysis presented earlier, we find the flux density that will produce $S/N \geq 5$ is

TABLE 1
PARAMETERS OF THE ETA SEARCH

Parameter	Value
Observing frequency (ν)	38 MHz
Single dipole collecting area (A)	18.8 m ²
Beam solid angle (Ω)	2.6 sr
Number of dipoles (N_{dipoles})	4
System temperature (T_{sys})	6000 K
Processed bandwidth (B)	3.75 MHz
Minimum integration time (τ_{min})	9.97 ms
Frequency channel width ($\Delta\nu$)	7.32 kHz

$$f_{\nu} \gtrsim 5 \frac{kT_{\text{sys}}}{A\sqrt{B\Delta t_{\text{pulse}}}} \frac{1}{\sqrt{N_{\text{dipoles}}}}. \quad (28)$$

For the observing parameters in Table 1, the required pulse flux density is given by

$$f_{\nu} \gtrsim 570 \text{ Jy} \left(\frac{\Delta t_{\text{pulse}}}{1 \text{ s}}\right)^{-1/2}. \quad (29)$$

ETA is strongly noise limited by Galactic synchrotron emission, as opposed to any internal or terrestrial noise, as demonstrated by Ellingson et al. (2007) and Deshpande (2009). In addition, Ellingson et al. (2007) demonstrated the basic functionality of ETA obtaining observations that showed the expected frequency dependence of the total received power and the diurnal variation of total received power from the Galaxy, extrapolating from the 408 MHz Sky Survey of Haslam et al. (1982).

Removal of the instrumental frequency response yields an estimate of the power spectral density S_{sky} at the antenna terminals, which can be converted into a temperature via $S_{\text{sky}} = e_r k T_{\text{sky}} \Delta\nu$, where k is Boltzmann’s constant, e_r is the loss due to the finite conductivity of the materials used to make the antenna as well as the absorption by the imperfect (non-perfectly conducting) ground, and $\Delta\nu$ is the spectral resolution bandwidth (Ellingson et al. 2007). The expected value of T_{sky} is given by the Rayleigh–Jeans approximation,

$$T_{\text{sky}} = \frac{1}{2k} I_{\nu} \frac{c^2}{\nu^2}. \quad (30)$$

From observations of the Galactic polar region carried out by Cane (1979), we assume

$$I_{\nu} = I_g \left(\frac{\nu}{\text{MHz}}\right)^{-0.52} + I_{eg} \left(\frac{\nu}{\text{MHz}}\right)^{-0.80}, \quad (31)$$

where $I_g = 2.48 \times 10^{-20}$ and $I_{eg} = 1.06 \times 10^{-20}$.

⁵ ETA is a joint project between the Bradley Department of Electrical and Computer Engineering and the Department of Physics at Virginia Polytechnic Institute and State University (Ellingson et al. 2007).

3.4. Data Reduction

We performed a single-dispersed-pulse search as described by Cutchin (2011) and Cordes & McLaughlin (2003). As discussed in detail above, a radio pulse is dispersed as it propagates through the ionized interstellar medium (ISM) or the intergalactic medium (IGM). The magnitude of this effect is quantified by the dispersion measure (DM), which is the integral of the electron column density along the path of propagation. For example, a signal from a pulsar out of the plane of the Galaxy with a $DM \sim 30 \text{ pc cm}^{-3}$ would experience a delay of $\sim 90 \text{ s}$ at 38 MHz. The delay scales as the inverse square of the observing frequency, making it greater at lower frequencies. The DM of a new source or transient is not known a priori, therefore a dedispersion search is performed over many candidate DMs. The data were incoherently dedispersed across 1153 trial DMs in the range $10\text{--}100 \text{ pc cm}^{-3}$, with a DM spacing $\delta DM = 0.002 \text{ DM}$, and searched over multiple assumed pulse widths in the range $10 \text{ ms--}2 \text{ s}$. Dedispersion searching has proven effective for the detection of giant pulses, rotating radio transients (RRATs; McLaughlin et al. 2006), and the recently detected fast radio bursts (FRBs; Thornton et al. 2013). The dedispersed time series are smoothed with a range of integration times to search for pulses matched in duration to the integration time, which would yield the greatest signal-to-noise ratio for a pulse.

During these observations, no astrophysical transients were detected above the 5σ level. The frequency of spikes in the time series at the 5σ level was consistent with that expected from Gaussian noise. A representative plot of 1 hr of these

observations, confirming the expected Gaussian dependence of the background and the lack of astrophysical signals, is shown in Figure 1.

4. OBSERVATIONAL LIMITS ON PBH EXPLOSION RATE

The signal-to-noise ratio can now be calculated for various fireball Lorentz factors (γ_f) using the observing parameters in Table 1 and equation (27). To give an example result for discussion, we use the following nominal source parameters: $\eta = 0.01$ (or $\eta = 1$), an interstellar magnetic flux parameter of $b = 1$, and $DM = 30 \text{ pc cm}^{-3}$, which is appropriate for lines of sight with high Galactic latitudes (which would have the most beneficial S/N). Then, given the values in Table 1, the largest signal-to-noise ratio is for an explosion with

$$\gamma_f = 10^{4.3} \quad (32)$$

or $\gamma_{f5} = 0.199$ (See Fig. 2). In that case, the emitted pulse energy is $5.01 \times 10^{23} \text{ J}$, the critical frequency is 40.5 MHz, and the intrinsic pulse duration before any dispersion or scattering is about 25 ns. The resulting emitted pulse energy per frequency interval per steradian at 38 MHz is

$$I_{\nu\Omega} = 1.5 \times 10^{14} \text{ J Hz}^{-1} \text{ sr}^{-1}. \quad (33)$$

The observed pulse duration considering only dispersion broadening of the final detected pulse, using the nominal parameters for the PBH explosion, is $\Delta t_D = 0.066 \text{ s}$. Scatter

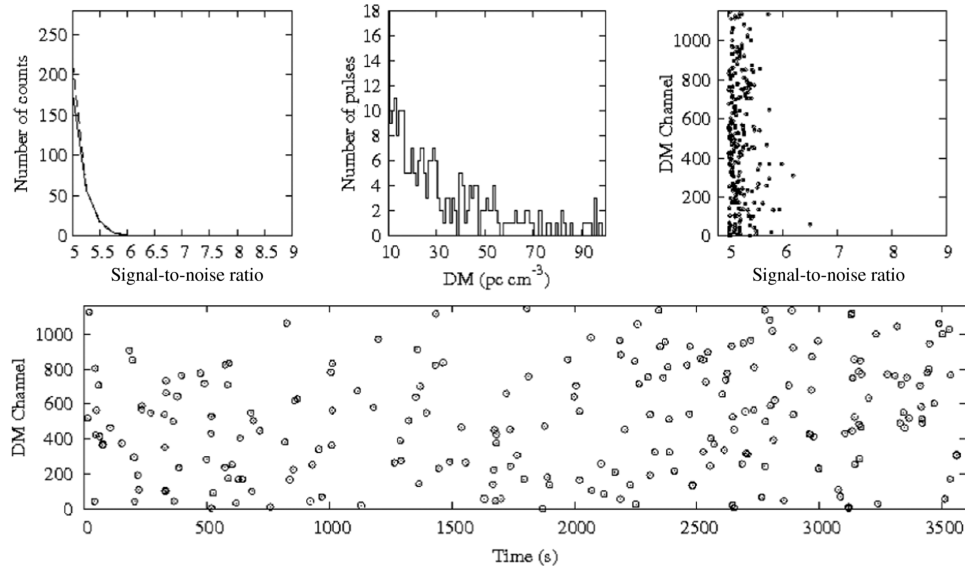


FIG. 1.—Representative plot of 1 hr of the observations conducted with the ETA. The upper left panel is histogram of S/N values. The *dashed curve* represents the number of pulses above a $S/N = 5$ due to noise alone, which is expected to follow a Gaussian distribution in the absence of any signal(s). The number of recorded pulses (*solid line*) does not clearly deviate from the expected number for a Gaussian process. The upper center plot is a histogram of the number of pulses across the DM values that were searched. The upper right plot shows no correlation between high S/N pulses and a particular DM channel. The bottom plot is a time series across the DM ranges searched. The size of the circular data points indicates the signal strength for each pulse.

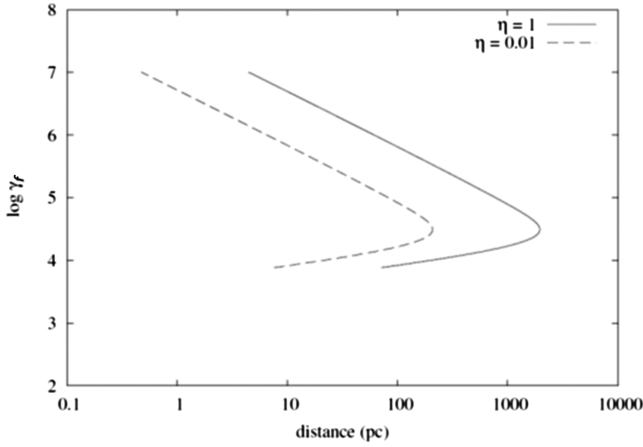


FIG. 2.—Distance to which a PBH explosion of $\eta = 0.01$ (dashed curve) and $\eta = 1$ (solid curve) can be detected for the range of possible fireball Lorentz factors is shown for the ETA with four dipoles. The detection threshold used is $S/N > 5$. The maximum detection distance is obtained for $\gamma_f = 4.3$.

broadening alone would produce an observed pulse duration of $\Delta t_{\text{scatt}} \approx 0.151$ s. Therefore, the observed pulse duration, including the combined interstellar broadening effects, is $\Delta t_{\text{obs}} = (\Delta t_D^2 + \Delta t_{\text{scatt}}^2)^{1/2} \approx 0.165$ s. Using equation (27) and the observation and source parameters noted above, we find that a PBH explosion can be detected with $S/N = 5$ to a distance of ~ 220 pc and 2.2 kpc for $\eta = 0.01$ (the topological phase transition) and $\eta = 1$ (the standard scenario), respectively.

The solid angle searched by an ETA dipole at any moment is $\Omega \approx 2.6$ sr at 38 MHz (Deshpande 2009). Therefore, the volume searched at any moment is $V = (1/3)d_{\text{max}}^3\Omega$ (Phinney & Taylor 1979), where d_{max} is the maximum distance to which such an explosion can be detected. If the observations are conducted over a time period T , then the upper limit to the rate r of PBH explosions, given no detections, is (Phinney & Taylor 1979)

$$r \approx \frac{1}{VT} = \frac{1.15}{d_{\text{max}}^3 T}. \quad (34)$$

For 4.15 hr of ETA observing, an upper limit on PBH explosions can be set at

$$r \approx \begin{cases} 2.3 \times 10^{-4} \text{ pc}^{-3} \text{ yr}^{-1} & \text{for } \eta = 0.01, \gamma_f = 10^{4.3} \\ 2.3 \times 10^{-7} \text{ pc}^{-3} \text{ yr}^{-1} & \text{for } \eta = 1, \gamma_f = 10^{4.3} \end{cases}. \quad (35)$$

These rate limits can be converted into limits on the current density of PBHs, Ω_{PBH} , as a fraction of the critical density, ρ_c . This can be done by relating the current PBH mass spectrum, $dN/dVdM$, to the current rate of PBH explosions, $dN/dVdt$, using

$$\frac{dN}{dVdM} = \left(\frac{dN}{dVdt} \right) \left(\frac{dt}{dM} \right), \quad (36)$$

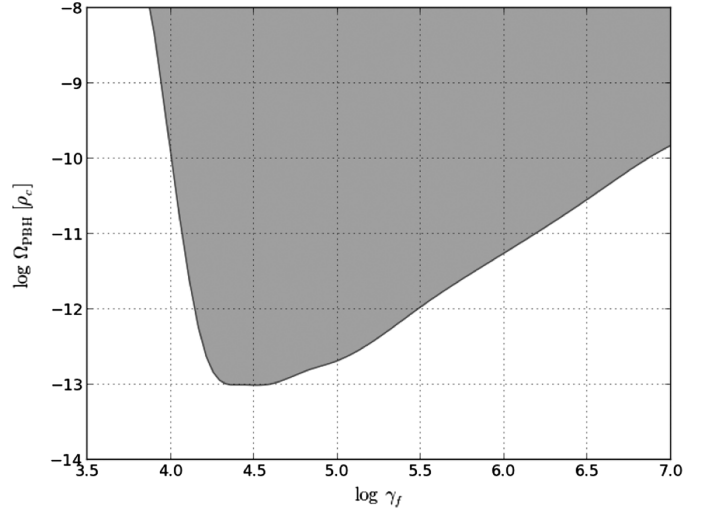


FIG. 3.—Limit on Ω_{PBH} vs. γ_f . The shaded region shows the section of parameter space defined by Ω_{PBH} and γ_f that is excluded by our search.

where dt/dM can be found by inverting equation (3). Carr (2005) has shown that the mass spectrum is directly related to Ω_{PBH} as

$$\frac{dN}{dVdM} = (\alpha - 2)(M/M_*)^{-\alpha} M_*^{-2} \Omega_{\text{PBH}} \rho_c, \quad (37)$$

where M_* is the current lower cutoff in the mass spectrum due to PBH evaporation, and $\alpha = 5/2$ for a radiation equation of state during the formation stage of PBHs. As described earlier, the Lorentz factor of the particles emitted by the PBH directly determines the volume searched and is thus directly related to the rate limit, which can be set by our observations. Thus, the relevant range of values for γ_f is related to different limits on Ω_{PBH} . Figure 3 shows the limit on Ω_{PBH} plotted versus γ_f , showing the region excluded by our observations. In the same way, our PBH rate density limit in the extra dimension scenario can be converted to a limit on Ω_{PBH} . Moreover, as noted in equation (8), the Lorentz factor is directly related to the compactification scale L . Thus, Figure 4 shows our limit on Ω_{PBH} plotted versus L , showing the region excluded by our observations.

5. DISCUSSION

The observations conducted by ETA, while lacking a positive detection of a radio transient, enable setting constraints on the rate of PBH explosions and the density of PBHs. These constraints, in turn, inform our understanding of the early universe and quantum gravity. Searches for PBHs serve as a direct probe of the spectrum of density perturbations in the early universe on a scale currently inaccessible to any other direct form of observation (Carr 2005). This provides crucial input to models of early cosmology, specifically those involving the inflationary paradigm (Carr 2005). Constraints on the topological phase

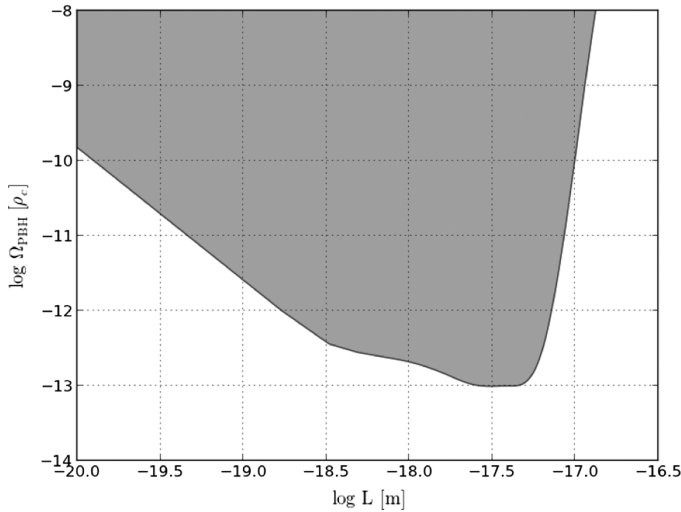


FIG. 4.—Limit on Ω_{PBH} vs. L . The shaded region shows the section of parameter space defined by Ω_{PBH} and L that is excluded by our search. This constrains the allowed compactification scale in extra-dimensional models. The excluded region would apply to extra-dimensional models that could be demonstrated to also lead generically to PBH production at the requisite mass scale when applied to early cosmology.

transition give important input into the allowed compactification scale in extra-dimensional models. Such results, while serving as a good complement to experimental results from accelerator-based searches for extra spatial dimensions, also probe a compactification scale that is inaccessible to even the most sensitive accelerator-based experiments. In the context of universal extra dimensions (UED), e.g., the bound set here improves upon the current threshold set by the Large Hadron Collider (LHC) by nearly an order of magnitude (Aad et al. 2012). However, it must be noted that this limits presupposes PBHs exist in the appropriate mass range. Thus, any limit would apply to extra-dimensional models that could be demonstrated to also lead generically to PBH production at the requisite mass scale, when applied to early cosmology.

We found an upper limit to the rate density of PBH explosions of $r \approx 2.3 \times 10^{-7} \text{ pc}^{-3} \text{ yr}^{-1}$ for the standard scenario. It is useful to compare this result with results from previous surveys. Typical rate limits for the results analyzed by Phinney and Taylor, at observing frequencies below $\sim 100 \text{ MHz}$, are $r \approx 10^{-6} \text{ pc}^{-3} \text{ yr}^{-1}$, where they assumed $\eta \approx 1$ and that PBHs are uniformly distributed throughout space (Phinney & Taylor 1979). Their analysis of observations from the Arecibo Observatory produced a rate limit $r \approx 2 \times 10^{-9} \text{ pc}^{-3} \text{ yr}^{-1}$. However, they assumed that the spectrum of a pulse from an exploding PBH is flat over the frequency range covered by their survey. Blandford's analysis (Blandford 1977) shows that this is not the case and that the spectrum falls dramatically above the critical frequency.

Using Blandford's spectrum (Blandford 1977) and the observational parameters from Phinney & Taylor (1979), we

determine a rate for these Arecibo observations paralleling the calculation detailed in § 4 for ETA. The only differences between the ETA analysis and the Arecibo analysis are: (1) $N_{\text{dipole}} = 2$ for Arecibo in equation (27), and (2) a careful analysis of equation (27) shows that the Arecibo observations are most sensitive to PBH explosions with $\gamma_f = 10^{4.6}$. The resulting upper limit to the rate of exploding PBHs is $r \approx 1.1 \times 10^{-8} \text{ pc}^{-3} \text{ yr}^{-1}$. The rate limit for $\gamma_f = 10^{4.3}$ is $4.8 \times 10^{-6} \text{ pc}^{-3} \text{ yr}^{-1}$, which is more than an order of magnitude less stringent than the rate limit presented for our observations, $r \approx 2.3 \times 10^{-7} \text{ pc}^{-3} \text{ yr}^{-1}$. The Arecibo observations had a duration of $\sim 300 \text{ hr}$, and our ETA observations had a duration of only 4.15 hr . That the search described here can set a stronger constraint for $\gamma_f = 10^{4.3}$ than the Arecibo observations is due in part to the fact that the critical frequency related to this fireball Lorentz factor is below the observing frequency of Arecibo. As noted above, the intensity for emission from a PBH explosion falls precipitously above the critical frequency. Thus, it is expected that instruments that observe at different frequencies should be most effective at probing different sections of the γ_f parameter space.

These points make manifest the relative merits of the two possible search strategies (large single dish with a small solid angle vs. an array of dipoles with a large solid angle), which is a primary motivation for the observations presented here. In the case of PBH explosions, the dipole array strategy is more efficient—particularly since future observations can easily expand upon the duration of observations with arrays such as LWA1 and LOFAR. Such instruments possess observational capabilities that the ETA lacks, including the ability to phase their dipole arrays to form beams and the ability to conduct all-sky imaging. The ability to form beams could be quite useful in searching for PBH explosions, even though such an observing strategy necessarily reduces the solid angle observed. This is because the increase in the distance observed would allow for an effective search of the Galactic halo while still retaining a relatively large observing solid angle. All-sky imaging could, in principle, be used to search for PBH explosions but is inherently more problematic because it can be very difficult to obtain the DM for an observed signal using such a method. Without this information, eliminating terrestrial-based signals becomes a greater challenge. Also, determining the DM of a signal allows for an estimate of the distance to the source, which in turn allows for a determination of the energy released by the source. This information is critical for establishing that the source was a PBH explosion and for distinguishing between the two PBH explosion scenarios described above.

It is also useful to compare these results with Benz & Paesold (1998), who utilize the spectrum from Blandford (1977) and take account of different possible γ_f for the expanding shell of charged particles. They are most sensitive for a PBH explosion with $\gamma_f \approx 10^{4.6}$, which they can detect, with $S/N > 5$ out to a distance of 70 pc . For the nominal source parameters noted

above and an effective observing time of 0.53 yr, the upper limit they set is $r = 4.8 \times 10^{-3} \text{ pc}^{-3} \text{ yr}^{-1}$ for $\eta \approx 1$ and $\gamma_f \approx 10^{4.6}$, assuming that PBHs are uniformly distributed throughout space. The observations presented here set a more stringent constraint for all possible values of γ_f , with only ≈ 4 hr of observing.

It has been suggested that PBHs may contribute to the dark matter in our Galaxy (MacGibbon & Carr 1991; Ivanov et al. 1994; Afshordi et al. 2003; Seto & Cooray 2004; Abramowicz et al. 2009). PBHs would, therefore, not be uniformly distributed throughout space, but would be clumped together in the halos of galaxies (Wright 1996; Abramowicz et al. 2009; Lehoucq et al. 2009). Lehoucq et al. (2009) used whole-sky survey data obtained by the Energetic Gamma-Ray Experiment Telescope (EGRET) to calculate the PBH explosion rate. They assumed PBHs to be distributed as dark matter and to have an initial mass $M = 5 \times 10^{14} \text{ g}$. By comparing the predicted cumulative Galactic gamma-ray emission to the one observed

by the EGRET satellite, they found an upper limit to the local rate of PBH explosions ($\eta = 1$) to be $\approx 0.059 \text{ pc}^{-3} \text{ yr}^{-1}$. The limit calculated in the current work, using similar assumptions, is about 5 orders of magnitude lower.

We thank Andy O'Bannon for a thorough and insightful reading of this manuscript and Jamie Tsai for thoughtful commentary. Part of this research was carried out while the primary author held a National Research Council (NRC) Postdoctoral Research Appointment at the U.S. Naval Research Laboratory (NRL). M. Kavic and A. Larracuenta were supported by NASA Grant NNX11AI27G. Construction and operation of ETA were supported through an NSF Advanced Techniques and Instrumentation (ATI) grant No. AST-0504677 and was hosted at the Pisgah Astronomical Research Institute (PARI) near Balsam Grove, NC, from 2005 through 2008. Basic research in radio astronomy at NRL is supported by 6.1 base funding.

REFERENCES

- Aad, G., et al. 2012, *Phys. Lett. B*, 718, 411
- Abramowicz, M. A., Becker, J. K., Biermann, P. L., Garzilli, A., Johansson, F., & Qian, L. 2009, *ApJ*, 705, 659
- Afshordi, N., McDonald, P., & Spergel, D. 2003, *ApJ*, 594, L 71
- Balsano, R., et al. 1996, in *AIP Conf. Proc.* 384, 3rd Huntsville Symp. on Gamma-Ray Bursts, eds. C. Kouveliotou, M. F. Briggs, & G. J. Fishman (New York: AIP), 575
- Barrau, A., Rovelli, C., & Vidotto, F. 2014, *Phys. Rev. D*, 90, 127503
- Benz, A. O., & Paesold, G. 1998, *A&A*, 329, 61
- Blandford, R. D. 1977, *MNRAS*, 181, 489
- Broniowski, W., Florkowski, W., & Glozman, L. Y. 2004, *Phys. Rev. D*, 70, 117503
- Cane, H. V. 1979, *MNRAS*, 189, 465
- Carr, B. J. 2005, in *59th Yamada Conf. on Inflating Horizon of Particle Astrophysics and Cosmology* (Tokyo, Japan: Universal Academy Press Inc. and Yamada Science Foundation), 129
- Cohen, T. D., & Krejcirik, V. 2012, *J. Phys. G*, 39, 055001
- Cordes, J. M., & McLaughlin, M. A. 2003, *ApJ*, 596, 1142
- Cordes, J. M., & Rickett, B. J. 1998, *ApJ*, 507, 846
- Cutchin, S. E. 2011, Ph.D. thesis, Virginia Polytechnic Inst. and State Univ.
- Deshpande, K. 2009, M.S. thesis, Virginia Polytechnic Inst. and State Univ.
- Ellingson, S. W., Simonetti, J. H., & Patterson, C. D. 2007, *IEEE Trans. Antennas Propag.*, 55, 826
- Gregory, R., & Laflamme, R. 1993, *Phys. Rev. Lett.*, 70, 2837
- Haslam, C., Salter, C., Stoffel, H., & Wilson, W. 1982, *A&AS*, 47, 1
- Hawking, S. W. 1975, *Commun. Math. Phys.*, 43, 199
- Ivanov, P., Naselsky, P., & Novikov, I. 1994, *Phys. Rev. D*, 50, 7173
- Jelley, J., Fruin, J., Porter, N., Weekes, T. C., Smith, F. G., & Porter, R. A. 1965, *Nature*, 205, 327
- Kavic, M., Simonetti, J. H., Cutchin, S. E., Ellingson, S. W., & Patterson, C. D. 2008, *J. Cosmol. Astropart. Phys.*, 0811, 017
- Kol, B. 2002, preprint (hep-ph/0207037)
- Lehoucq, R., Cassé, M., Casandjian, J.-M., & Grenier, I. 2009, *A&A*, 502, 37
- MacGibbon, J. H., & Carr, B. J. 1991, *ApJ*, 371, 447
- McLaughlin, M. A., et al. 2006, *Nature*, 439, 817
- Meikle, W. P. S., & Colgate, S. A. 1978, *ApJ*, 220, 1076
- Page, D. N., & Hawking, S. W. 1976, *ApJ*, 206, 1
- Phinney, S., & Taylor, J. H. 1979, *Nature*, 277, 117
- Porter, N., Long, C., McBreen, B., Murnaghan, D., & Weekes, T. 1965, in *Proc. 9th Int. Cosmic Ray Conf.*, Vol. 2 (London: Inst. Physics and Physical Society), 706
- Rees, M. J. 1977, *Nature*, 266, 333
- Seto, N., & Cooray, A. 2004, *Phys. Rev. D*, 70, 063512
- Stappers, B., et al. 2011, *A&A*, 530, A 80
- Taylor, G. B., et al. 2012, *J. Astron. Instrum.*, 1, 1250004
- Thornton, D., et al. 2013, *Science*, 341, 53
- Tingay, S., et al. 2013, *Proc. Astron. Soc. Australia*, 30, e007
- Wright, E. L. 1996, *ApJ*, 459, 487